INPE – National Institute for Space Research
São José dos Campos – SP – Brazil – May 16-20, 2016

ANALYSIS OF A TEMPERATURE DEPENDENT SMA-PENDULUM SYSTEM

Dimitri D. A. Costa[1], Marcelo A. Savi[2]

[1]COPPE - Department of Mechanical Engineering, Rio de Janeiro, Brazil, dda.costa@mecanica.coppe.ufrj.br
[2]COPPE - Department of Mechanical Engineering, Rio de Janeiro, Brazil, savi@mecanica.ufrj.br

Abstract: Pendulum is a simple system that is usually related to great discoveries in technology and science. Nonlinear dynamics of pendulum systems enable a variety of responses being the objective of studies of oscillations, bifurcations and chaos. Smart material nonlinear effects are employed in several applications due to their adaptive behavior presenting great advantages in control strategies. This work deals with the dynamics of an SMA-pendulum system that consists of a pendulum coupled with shape memory alloy springs. Temperature dependent behavior of the SMA is explored, presenting complex responses and the possibility of thermal control of the system.

keywords: Bifurcation Analysis and Applications, Control of Chaos, Chaos and Global Nonlinear Dynamics.

1. INTRODUCTION

Pendulum systems are extensively analyzed due to a variety of reasons, being a source of motivation for several discoveries in nonlinear dynamics and other fields of engineering. De Paula *et. al.* [1] discussed some aspects of pendulum dynamics, presenting an experimental-numerical investigation of a typical mechanical apparatus. Results show several complex responses that include bifurcations, chaos and transient chaos. Nonlinear control of these systems are investigated in several references, and it should be highlighted the use of either fuzzy logic or chaos control approaches [2]–[4]. Pendulum-like systems are also employed to model biological systems as Suzuki *et. al.* [5] that models the control of an ankle. Motor system analysis also uses pendulum systems as Chen *et. al.* [6] that treated the control of induction motors for electrical vehicles. Ju *et. al.* [7] also used pendulum system to model cranes and their swings.

Smart materials represent a class of advanced materials with remarkable properties conferred by the coupling between different physical fields. Usually, they are employed for control purposes due to their adaptive capacity. Shape memory alloys (SMAs) belong to the smart materials class, being widely applied in vibration control [8], origami structures [9], robotics [10] and energy harvesting [11], showing a broad use and potential for numerous applications. Their unique behavior is due to the thermoelastic martensitic transformations that imply some of their traditional effects as pseudoelasticity and shape memory effect. The first one is identified as a complete strain recovery of the material with a large hysteresis in a loading-unloading cycle. On the other hand, shape memory effect is the ability to completely recover an amount of residual strain after a proper themomechanical loading process. These characteristics can be used to mimic biological movements, robotics, aerospace engineering, shape and vibration control, among others [9]–[13]. Synergistic use of smart materials has been increasing, by exploring the proper characteristics of each material involved. SMA-piezoelectric systems are good examples for enhance energy harvesting capacity combining different characteristics of smart materials [11], [14]–[16].

This work deals with the nonlinear dynamics of an SMA-Pendulum system composed of a nonlinear pendulum coupled with SMA springs. This system has adaptive behavior, presenting a temperature dependent response. Dynamical investigation is carried out pointing to some advantages of the use of SMA elements as well as some possible applications.

2. SMA-PENDULUM SYSTEM

The SMA-pendulum system is an apparatus described by De Paula *et al.* [1] except that the linear springs are replaced by SMA springs. It is a disc with diameter D with a concentrated mass m. The excitation of the pendulum is provided by a DC motor, with an arm of length b, connected to string-spring system.

By considering that ϕ is the angle of the pendulum, and assuming that the dissipation is a combination of linear viscous and dry friction, the equation of motion is given by:

$$\phi'' = -\frac{\vartheta}{I\omega_0}\phi' - \frac{\mu}{mgD}\operatorname{sgn}(\phi') - \frac{\sin(\phi)}{2} + \frac{d}{2mgD}(F_m - s_m) \tag{1}$$

with,

$$t^* = t\omega_0\,,\ \ \omega_0 = \sqrt{\frac{mgd}{I}} \tag{2}$$

where a is the distance between the center of the disc and the center of the rotor, μ is the dry damping coefficient, ϑ is the viscous damping coefficient, ω is the rotor frequency, I is the angular inertia of the pendulum, g is the acceleration of gravity, t is the time, t^* is a dimensionless time, ω_0 is a reference frequency, s_m is the force of the anchored spring and F_m is the excitation force of the spring and motor system. The superscript $(\ )'$ corresponds to dimensionless time derivative.

The geometric displacement due to the movement of the motor can be written as:

$$y = \sqrt{\left(a^2 + b^2 - 2abcos\left(\frac{\omega t^*}{w_0} + \theta\right)\right)} - (a-b) - \frac{d\phi}{2} \tag{4}$$

where θ is the initial phase of the motor.

Different constitutive models can describe the thermomechanical behavior of SMAs. For the sake of simplicity, a polynomial model is employed following the stress-strain (σ-ε) relation given by,

$$\sigma = a_m^*(T - T_M)\varepsilon - b_m^*\varepsilon^3 + \frac{{b_m^*}^2}{a_m^*(T_A - T_M)}\varepsilon^5 \tag{5}$$

where a_m^* and b_m^* are material parameters, T_M is the temperature below which only martensitic phase is stable, T_A is the temperature above which only austenitic phase is stable (at stress free scenario), T is the temperature. Based on that, and assuming that phase transformation is homogeneous for the spring cross-section, it is possible to write a force-displacement equation for the spring that is similar to stress-strain expression [17], [2,

$$F_m = a_m(T - T_m)y\ - b_m y^3 + \frac{{b_m}^2}{a_m(T_A - T_m)}y^5 \tag{6}$$

$$s_m = a_m(T - T_m)\frac{\phi d}{2} - b_m\left(\frac{\phi d}{2}\right)^3 + \frac{{b_m}^2}{a_m(T_A - T_m)}\left(\frac{\phi d}{2}\right)^5 \tag{7}$$

3. NUMERICAL SIMULATIONS

Numerical simulations are performed to investigate the nonlinear dynamics of the SMA-pendulum system. Fourth-order Runge-Kutta method is employed. The parameters used are the following: $m = 1.47$ kg, $D = 9.5$ cm, $d = 4.8$ cm, $b = 6$ cm, $a = 16$ cm, $\mu = 1.272\ 10^{-4}$ Nm, $\vartheta = 2.368\ \frac{\mathrm{kgm^2}}{\mathrm{s}}$, $g = 9.81\ \mathrm{m/s^2}$. SMA parameters are matched with experimental data to emulate a real SMA spring: $T_A = 289.35$ K, $T_M = 282.45$ K, $a_m = 0.4375$ N/mK and $b_m = 150$ Pa/m.

Initially, the structure of equilibrium points is analyzed, giving special attention to its temperature dependent behavior. In this regard, the system is not subjected to excitation and therefore, the motor is at rest in a specific angle θ. A locus of equilibrium points against the forcing motor phase is plotted. The stability of each equilibrium point is analyzed assessing the eigenvalues of the Jacobian matrix. A reference situation is defined at high temperature where results are similar to the one obtained with an elastic spring and discussed in [1]. This situation is simulated considering T = 291.15 K. Figure 1 shows the equilibrium point locus for this case presenting regions related to just only one stable equilibrium point and a region $(2.71 \le \theta \le 4.11)$ related to three equilibrium points (two stable and one unstable).

The influence of temperature on the structure of equilibrium point is now in focus considering the system response for different temperatures. The introduction of SMA spring promotes dramatic changes on system responses. Figures 2a and 2b show situations where $T < T_M$. Note that there are five equilibrium points for $\theta = 0$, two of them unstable and three stable, all positioned symmetrically around the origin. By changing the motor's phase, the symmetry is broken moving the equilibrium points until stable and unstable equilibrium points collide. It should be observed that the asymmetries on the system are introduced by the motor's phase angle θ. The increase of temperature changes the structure of equilibrium points making the ellipse grow Figure 3d until the end touch on Figure 3a where $T_M < T < T_A$. This intermediate temperature range allows both martensite and austenite to be stable and therefore, is related to a greater equilibrium point structure. The increase of temperature for higher levels promotes the creation of another ellipse as shown in Figure 3b. By increasing even more the temperature, the ellipse growth is observed until it breaks, that is followed by the creation of another ellipse (Figure 3c). A new dramatic change occurs when temperature values approach T_A (Figure 3d). After this value, only austenite is stable in a stress-free state. Note that most extreme stable equilibrium point breaks into three, one stable and one ellipse structure of stable and unstable points. At this point the ellipse structures start to contract and form by the coalescences of stable and unstable paths of equilibrium points. Note that the ellipses can be formed as single, pairs or divide while collapsing (Figures 4). The limit case occurs at $T = 291.15$ K where constitutive nonlinearity can be neglected and the original case presented in Figure 1 is reproduced.

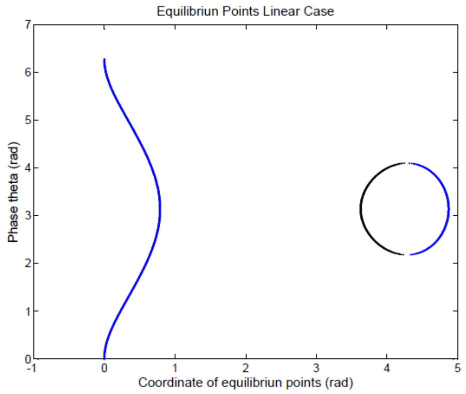

Figure 1 – Location of equilibrium points in rad against forcing motor phase in rad for the linear case. Stable points are in gray (blue) and unstable in black.

Forced vibration of the system is now analyzed. Initially, bifurcation diagrams are of concern providing a general comprehension about the system dynamics. Diagrams are constructed eliminating the first 600 periods and different initial conditions. Parameter b is changed to be 1.5 cm, reducing the energy delivered to the system. Note that the change on temperature causes different kinds of responses. Periodic and chaotic responses are possible and multistability can be observed since different initial conditions are related to different solutions.

Figure 5 shows the influence of temperature variation as some of the bifurcation diagrams traced from $T = 284.55$ K to $T = 286.15$ K, with a 0.5 K interval. There are always two or more coexisting orbits, one of them always been a periodic one. Besides, two chaotic regions coexist on Figure 5b. The increase of temperature causes the chaotic regions creation, moving to the left and vanishing. The chaotic region on the bottom of Figure 5c and 5d also have islands of periodicity that also evolve with the chaos, "pushing" it aside and rising and growing between it. Therefore, a temperature increase can be related to the appearance of periodic islands dislocating or destroying the chaotic regions.

This temperature dependent behavior can be exploited for control purposes. Figure 6 illustrates a situation where temperature variation is employed to change the system global response. It is built by initializing the system at $x_0 = (6\,\text{rad}, 0\,\text{rad/s})$, forcing frequency of 6.5 rad/s and maintaining T=285.15 K for 600 cycles. Under this condition, the system presents a chaotic response (upper attractor of Figure 5b). Afterward, the temperature is increased by a ramp function with linear coefficient 0.1 K/s, until it reaches $T = 287.15\,K$, a temperature approaching T_A, related to a period-1 response. After 1000 cycles the temperature is decreased to T = 286.65 K, making the period-1 response unstable (response around 6 rad on Figure 5d) and pushing the system to another period-1 response. It is also possible to make a chaotic-periodic-chaotic control with other temperatures and initial conditions.

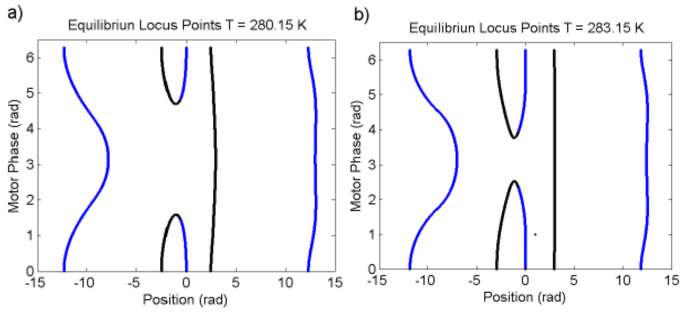

Figure 2 – Location of equilibrium points in rad against forcing motor phase in rad for the SMA spring on temperatures below (a) and right above T_m (b). Stable points are in gray (blue) and unstable in black. a) 280.15 K b) 283.15 K.

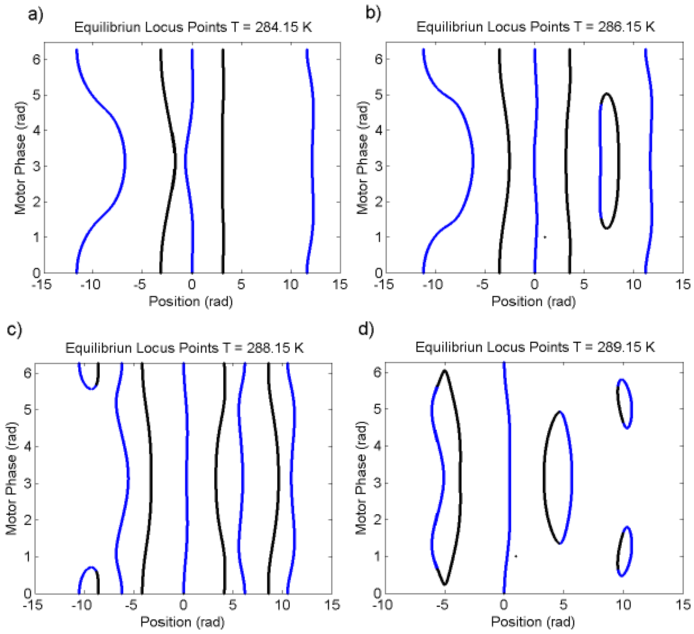

Figure 3 – Location of equilibrium points in rad against forcing motor phase in rad for the SMA spring system case on $T_m < T < T_A$. Stable points are in gray (blue) and unstable in black. a) 284.15 K b) 286.15 K c) 288.15 K d) 289.15 K

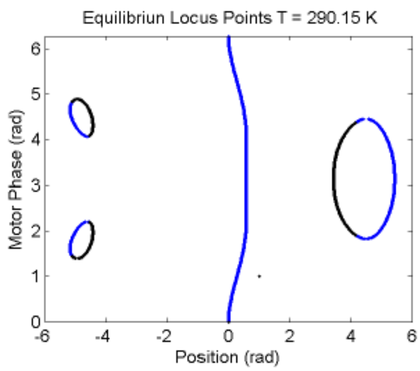

Figure 4 – Location of equilibrium points in rad against forcing motor phase in rad for the SMA spring system case on $T > T_A$. Stable points are in gray (blue) and unstable in black.

3. CONCLUSION

This work deals with the nonlinear dynamics of an

SMA-pendulum. The use of SMA element provides a temperature dependent behavior introducing several possibilities related to system response. The structure of equilibrium points is discussed showing a large number of points with complex behavior altered by temperature. Concerning forced vibration, the system presents several responses that can be exploited for control purposes, as temperature variations can be employed to change either the system position or the system response type in a variety of ways. These situations are demonstrated by chaotic-periodic transitions.

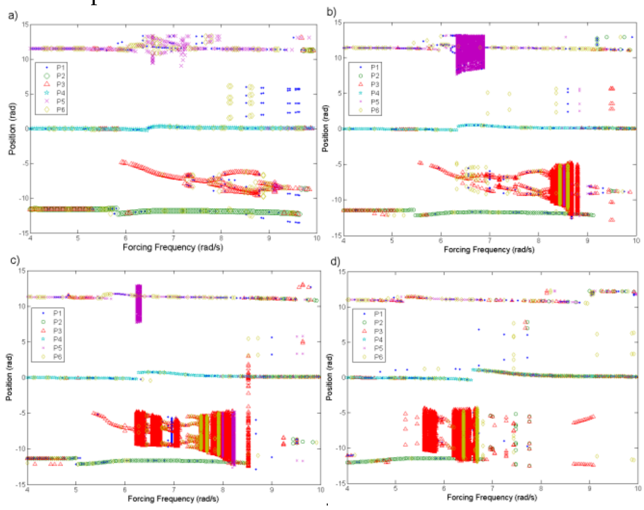

Figure 5 – Evolution of the chaotic region through different temperatures with a short motor's arm length b=1.5 cm. a) At 284.65K, b) at 285.15 K, c) at 285.65 K, d) at 286.65 K. Only the results of the most relevant points are shown for simplicity, other initial condition only presents the same trends of the other 6.

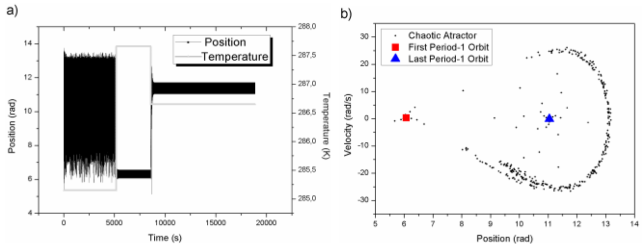

Figure 6 – Orbits with change in temperature. a) Chaotic-periodic-periodic cycle. b) Poincaré section of the chaotic attractor and periodic orbits.

ACKNOWLEDGMENTS

The authors would like to acknowledge the support of the Brazilian Research Agencies CNPq, CAPES, FAPERJ as well as INCT-EIE (National Institute of Science and Technology - Smart Structures in Engineering). The acknowledgement applies also to Air Force Office of Scientific Research (AFOSR).

References

[1] A. S. de Paula, M. A. Savi, e F. H. I. Pereira-Pinto, "Chaos and transient chaos in an experimental nonlinear pendulum", J. Sound Vib., vol. 294, nº 3, p. 585–595, jun. 2006.

[2] W. M. Bessa, A. S. de Paula, e M. A. Savi, "Chaos control using an adaptive fuzzy sliding mode controller with application to a nonlinear pendulum", Chaos Solitons Fractals, vol. 42, nº 2, p. 784–791, out. 2009.

[3] A. S. de Paula e M. A. Savi, "Controlling chaos in a nonlinear pendulum using an extended time-delayed feedback control method", Chaos Solitons Fractals, vol. 42, nº 5, p. 2981–2988, dez. 2009.

[4] Y. Pan, Y. Zhou, T. Sun, e M. J. Er, "Composite adaptive fuzzy H∞ tracking control of uncertain nonlinear systems", Neurocomputing, vol. 99, p. 15–24, jan. 2013.

[5] Y. Suzuki, T. Nomura, M. Casadio, e P. Morasso, "Intermittent control with ankle, hip, and mixed strategies during quiet standing: A theoretical proposal based on a double inverted pendulum model", J. Theor. Biol., vol. 310, p. 55–79, out. 2012.

[6] L. Chen, X. Sun, H. Jiang, e X. Xu, "A High-Performance Control Method of Constant -Controlled Induction Motor Drives for Electric Vehicles", Math. Probl. Eng., vol. 2014, p. 1–10, 2014.

[7] F. Ju, Y. S. Choo, e F. S. Cui, "Dynamic response of tower crane induced by the pendulum motion of the payload", Int. J. Solids Struct., vol. 43, nº 2, p. 376–389, jan. 2006.

[8] W. M. Bessa, A. S. de Paula, e M. A. Savi, "Adaptive fuzzy sliding mode control of smart structures", Eur. Phys. J. Spec. Top., vol. 222, nº 7, p. 1541–1551, set. 2013.

[9] K. Kuribayashi, K. Tsuchiya, Z. You, D. Tomus, M. Umemoto, T. Ito, e M. Sasaki, "Self-deployable origami stent grafts as a biomedical application of Ni-rich TiNi shape memory alloy foil", Mater. Sci. Eng. A, vol. 419, nº 1–2, p. 131–137, mar. 2006.

[10] B. Kim, M. G. Lee, Y. P. Lee, Y. Kim, e G. Lee, "An earthworm-like micro robot using shape memory alloy actuator", Sens. Actuators Phys., vol. 125, nº 2, p. 429–437, jan. 2006.

[11] G. A. Lebedev, B. V. Gusarov, B. Viala, J. Delamare, O. Cugat, T. Lafont, e D. I. Zakharov, "Thermal energy harvesting using shape memory/piezoelectric composites", in Solid-State Sensors, Actuators and Microsystems Conference (TRANSDUCERS), 2011 16th International, 2011, p. 669–670.

[12] L. G. Machado, M. A. Savi, e P. M. C. L. Pacheco, "Nonlinear dynamics and chaos in coupled shape memory oscillators", Int. J. Solids Struct., vol. 40, nº 19, p. 5139–5156, set. 2003.

[13] L. G. Machado e M. A. Savi, "Medical applications of shape memory alloys", Braz. J. Med. Biol. Res., vol. 36, nº 6, p. 683–691, 2003.

[14] A. C. Cellular e M. A. Savi, "On the influence of nonlinear mechanical effects on vibration-based energy harvesting", apresentado em International Congress of Mechanical Engineering, Rio de Janeiro, 2015.

[15] A. F. Arrieta, P. Hagedorn, A. Ertuk, e D. J. Inman, "A piezoelectric bistable plate for nonlinear broadband energy harvesting", Appl. Phys. Lett., vol. 97, nº 10, 2010.

[16] L. L. Silva, S. A. Oliveira, P. M. L. C. Pacheco, e M. A. Savi, "Synergistic Use of Smart Materials for Vibration-Based Energy Harvesting", Eur. Phys. J. – Spec. Top., vol. 224, nº 14–15, p. 3005–3012, 2015.

[17] R. A. A. Aguiar, M. A. Savi, e P. M. C. L. Pacheco, "Experimental and numerical investigations of shape memory alloy helical springs", Smart Mater. Struct., vol. 19, nº 2, p. 025008, fev. 2010.